Desalination and Water Treatment
www.deswater.com
doi: 10.1080/19443994.2013.806999

52 (2014) 1654–1661
February

Taylor & Francis
Taylor & Francis Group

Liquid film evaporation enhancement in a vertical annulus with preheated air flow

R. Ben Radhia[a], S. Harmand[b], J.P. Corriou[c], S. Ben Jabrallah[a,d,*]

[a]*Laboratoire d'énergétique et des Transferts thermique et massique, Campus Universitaire 1060, Tunis, Tunisia*
[b]*Université de Lille Nord de France, F-59000 Lille UVHC/TEMPO, F-59313 Valenciennes Cedex, France*
[c]*Laboratoire Réactions et Génie des Procédés, CNRS-ENSIC-Lorraine Université, 1, rue Grandville, B.P. 54001 Nancy, Cedex, France*
[d]*Faculté des Sciences de Bizerte, Université de Carthage 7021 Bizerte, Tunisia*
Tel. +216 98 486 708; email: sadok.jabrallah@fsb.rnu.tn

Received 19 December 2011; Accepted 2 October 2012

ABSTRACT

The evaporation by mixed convection of a water film falling down the inner wall of a vertical annulus was studied numerically. The outer wall was assumed to be insulated and dry. A counter-current flow of preheated, dry air was blown between two concentric cylinders. This air flow was preheated at the inlet of the annulus, which allowed for the evaporation phenomenon. The governing equations for the gas flow were solved using the finite volume method. The energy and mass balances for an element of liquid film allowed us to calculate the average temperature of the liquid film and the evaporated average mass flux density. The influence of the air flow and water film parameters on the evaporated average mass flux density was studied. The increase in this density was obtained by either increasing the temperature and the velocity of air flow or by decreasing the vapour mass fraction at the inlet. The decrease of the mass flow rate and the temperature of feedwater caused an increase in the evaporation phenomenon. The curvature and the length also increased the heat and mass transfer for this annular geometry. These parameters are important factors for film evaporation enhancement in a vertical annulus.

Keywords: Evaporation; Liquid film; Air flow; Annulus

1. Introduction

Freshwater scarcity is a major problem for many countries. Faced with a shortage of drinking water, many developing countries seeking a simple and economically viable solution have turned to desalination of seawater. Two main technologies are used: membrane separation and distillation. Distillation is based on the phenomena of evaporation and condensation. In this paper, evaporation and condensation were considered separately to limit the complexity of the problem. The evaporation of a falling liquid film plays an important role in desalination systems.

*Corresponding author.

Presented at the Third Maghreb Conference on Desalination and Water Treatment (CMTDE 2011) Hammamet, Tunisia, 18–22 December 2011

There is need for better understanding of the complex interaction between heat and mass transfer encountered in both evaporation and condensation. Many past investigations focused on evaporation; however, most of them considered only the gas vapour, as the film has a very low mass flow rate; thus, the wall was assumed to be wetted and the film was regarded as a boundary condition for heat and mass transfer. In this context, the evaporation of liquid film has been studied for many different geometries, some of which are described below.

The case of a vertical channel is widely investigated. A numerical study of heat and mass transfer by laminar mixed convection between two parallel plates with asymmetric heating was performed by Yan et al. [1]. They demonstrated that the transport of latent heat is the dominant transfer mechanism along the wetted walls. A numerical study of water evaporation in dry air, humid air and superheated steam in a vertical channel was conducted by Debbissi et al. [2]. Ait Hammou et al. [3] numerically studied the simultaneous heat and mass transfer in a vertical channel with two wetted, isothermal walls. They conducted a parametric study of air flow to determine the nature of the phenomena taking place in the channel. Yan et al. [4] examined heat and mass transfer in a vertical annulus driven by mixed convection. The inner and the outer walls of the annulus are kept at elevated, uniform temperatures T_1 and T_2, respectively. The evaluation of different heat fluxes are presented for cases which vary the Reynolds number, radii ratio and temperatures T_1 and T_2. The same geometry was used in a later study by Yan et al. [5] assuming natural convection alone. The heat and mass transfer along the two walls are performed in detail. They demonstrated that the heat transfer along the gas–liquid interface is dominated by the transport of latent heat. Jang et al. [6] conducted a numerical study of heat transfer enhancement of film evaporation in inclined square ducts under mixed convection. In this study, the air flow was considered steady and three-dimensional, and they demonstrated that the system that operated with high first wall temperatures enhanced the heat transfer. Fahem et al. [7] studied evaporation in a cavity. They simultaneously solved the equations describing the solid of the heated wall, the falling liquid film and the gas. The evaporation of a binary film on the external wall of the inner tube of a vertical annulus was proposed by El Armouzi et al. [8]. They proposed an analytic expression for the liquid film velocity and demonstrated that both heat and mass transfer were more significant at the inlet of the annulus and increase with the heat flux density. Feddaoui et al. [9] numerically studied heat and mass transfer in a vertical heated tube that had been subjected to mixed convection. They demonstrated that a larger heat and mass transfer was obtained for systems having large heat flux and a low Reynolds number. The numerical study of the heat and mass transfer with film evaporation in the channel that had a thermally insulated wall was conducted by Jang et al. [10]. The turbulent air flow was preheated and the liquid film was cooled. Particular attention was paid to the effect of the liquid film mass flow rate, Reynolds number and the hot air temperature. Evaporation and condensation in a rectangular cavity were examined by Ben Jabrallah et al. [11]. It was demonstrated that to increase the yield of fresh water, it is necessary to increase the heat flux density and the feedwater temperature, whereas decreasing the feedwater mass flow rate and reducing the wall temperature where condensation forms. Recently, Cherif et al. [12] experimentally and numerically studied the heat and mass transfer in a vertical channel. The liquid films fell on two walls heated by uniform heat flux densities. The other walls were assumed to be dry and adiabatic. The influence of heat flux density and air flow velocity on the heat and mass transfers was determined.

Previous works have studied the evaporation of liquid film in different configurations. Additionally, cases where the wall on which the liquid film flows was maintained at a uniform temperature or a uniform heat flux were widely investigated. These cases are often associated with desalination by solar energy, which has been described in previous works [13–15]. Because evaporation in an annular geometry with preheated air flow is poorly understood, we numerically solved this geometric configuration to investigate the evaporation of liquid film falling on the inner wall of the vertical annulus.

2. Problem statement

The problem under consideration is a vertical annulus with inner R_1 and outer R_2 radii equal to 2.5 and 4.6 cm, respectively. The length of the evaporator was $L = 1$ m. A liquid water film flows down the outer wall of inner tube. The opposite wall of the second tube is assumed to be dry and adiabatic. Dry air enters the annular domain with a uniform axial velocity u_0, temperature T_0 and vapour mass fraction c_0, as shown in Fig. 1. The liquid water film enters the inlet of the annulus with a mass flow rate F_{in} and a temperature T_{in}.

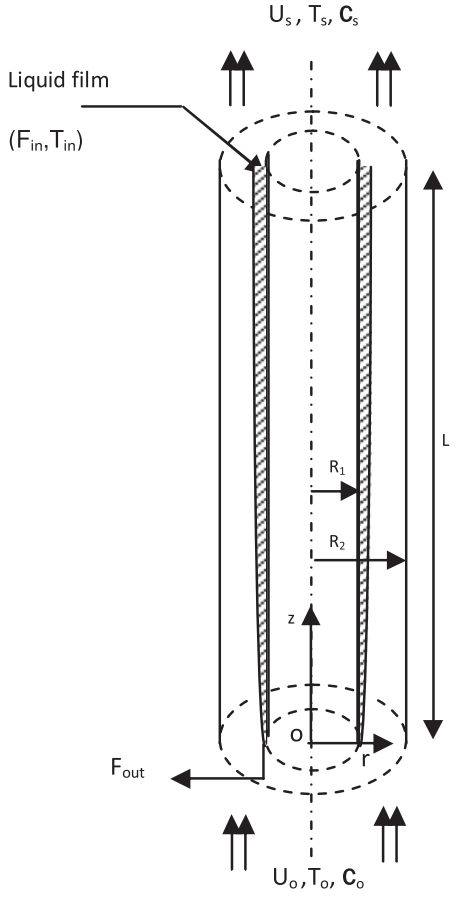

Fig. 1. Schematic representation of the physical system.

3. Model and assumptions

3.1. Gas phase

The following assumptions are adopted to describe the problem:

(1) The flow is two-dimensional gas phase.
(2) The Boussinesq assumption is valid.
(3) The flow is laminar and steady.
(4) The viscous dissipation and radiactive transfer are negligible.
(5) The Soret and Dufour effects are negligible.

The following equations are used for model development:

Continuity equation:

$$\frac{1}{r}\frac{\partial}{\partial r}(rv)+\frac{\partial}{\partial z}(u)=0 \tag{1}$$

Axial momentum equation:

$$\rho\left(v\frac{\partial u}{\partial r}+u\frac{\partial u}{\partial z}\right)=-\frac{\partial p}{\partial z}-(\rho-\rho_0)g+\mu\left[\frac{1}{r}\frac{\partial}{\partial r}\left(r\frac{\partial u}{\partial r}\right)+\frac{\partial^2 u}{\partial^2 z}\right] \tag{2}$$

Radial momentum equation:

$$\rho\left(v\frac{\partial v}{\partial r}+u\frac{\partial v}{\partial z}\right)=-\frac{\partial p}{\partial r}+\mu\left[\frac{1}{r}\frac{\partial}{\partial r}\left(r\frac{\partial v}{\partial r}\right)+\frac{\partial^2 v}{\partial z^2}\right]-\mu\frac{v}{r^2} \tag{3}$$

Energy equation:

$$\rho c_p\left(v\frac{\partial T}{\partial r}+u\frac{\partial T}{\partial z}\right)=\lambda\left[\frac{1}{r}\frac{\partial}{\partial r}\left(r\frac{\partial T}{\partial r}\right)+\frac{\partial^2 T}{\partial z^2}\right] \tag{4}$$

Concentration equation for water vapour:

$$v\frac{\partial C}{\partial r}+u\frac{\partial C}{\partial z}=D\left[\frac{1}{r}\frac{\partial}{\partial r}\left(r\frac{\partial C}{\partial r}\right)+\frac{\partial^2 C}{\partial z^2}\right] \tag{5}$$

3.2. Liquid film

In the literature, at the film inlet the liquid thickness is on the order of 10^{-4} m [16] because the liquid mass flow rate is assumed to be low. Consequently, the liquid thickness, δ, can be neglected, and the liquid film can be treated as one dimension. Additionally, the liquid flow was assumed to be laminar. To simplify the liquid film solution, we adopted the method elaborated by [11]. This method uses the conservation of mass and energy to calculate the radial average temperature, T_l, in an annular element of liquid film. It was assumed that the temperature and mass flow rate in the film depend only on z [17] as shown in Fig. 2.

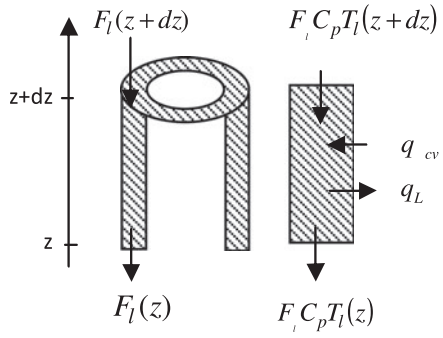

Fig. 2. Schematic representation of a liquid film element.

3.2.1. Mass balance

The conservation equations were written for an element of liquid film with a height of dz, a perimeter of $2\Pi R_1$ and a thickness of δ, as follows:

$$F_l(z+dz)2\Pi R_1 = F_l(z)2\Pi R_1 + m_v dz 2\Pi R_1 \quad (6)$$

and result in:

$$m_v = \frac{\partial F_l}{\partial z} \quad (7)$$

3.2.2. Energy balance

$$F_l(z+dz)C_{pl}\overline{T}_l(z+dz)_{/z+dz}2\Pi R_1 = F_l(z)C_{pl}\overline{T}_l(z)_{/z}2\Pi R_1 dz + m_v L_v 2\Pi R_1 dz + q_{cv}2\Pi R_1 dz \quad (8)$$

$$\frac{\partial}{\partial z}\left(F_l C_{pl}\overline{T}_l(z)\right) = \frac{\partial (F_l)}{\partial z}L_v + q_{cv} \quad (9)$$

3.3. Boundary conditions

3.3.1. In the liquid film

$$T_l(z=L) = T_{in} \quad F_l(z=L) = F_{in} \quad -\lambda_l\left(\frac{\partial T_l}{\partial r}\right)_{/r=R_1} = 0 \quad (10)$$

3.3.2. At the liquid–gas interface

$$u = u_{l,l} = u_I \quad T = T_{l,l} = T_I \quad \frac{\partial}{\partial z}\left(F_l C_{pl}\overline{T}_l(z)\right) = \frac{\partial (F_l)}{\partial z}L_v + q_{cv} \quad m_v = -\frac{\rho D}{1-c_I}\left(\frac{\partial c}{\partial r}\right)_I \quad (11)$$

The air–water interface was assumed to be at thermodynamic equilibrium. The air–vapour mixture is considered to be an ideal gas mixture, thus the mass fraction at the interface C_I can be evaluated by:

$$C_I = \frac{\frac{M_v}{M_a}}{\frac{P}{P_{vs}} + \frac{M_v}{M_a} - 1} \quad (12)$$

P_{vs} is the equilibrium vapour pressure and was calculated by the following expression:

$$\log_{10} P_{vs} = 28,5,905 - 8,2\log T + 2,480,410^{-3}T - \frac{3,142,32}{T} \quad (13)$$

3.3.3. In the gas phase

$$\text{At } r = R_2: \quad u = 0 \quad v = 0 \quad (14)$$

$$\text{At } z = L: \quad \frac{du}{dz} = 0 \quad \frac{dv}{dz} = 0 \quad \frac{dT}{dz} = 0 \quad \frac{dc}{dz} = 0 \quad (15)$$

$$\text{At } z = 0: \quad u = u_0 \quad v = 0 \quad T = T_0 \quad c = c_0 \quad (16)$$

3.4. Dimensionless modelling

The system describing the gas flow was transformed into a dimensionless form by adopting the following dimensionless variables:

$$U = \frac{u}{u_0} \quad V = \frac{vR_2}{v} \quad \eta = \frac{r}{R_2} \quad \zeta = \frac{2z(1-N)}{ReR_2} \quad N = \frac{R_1}{R_2} \quad C = \frac{c-c_0}{c_{in}-c_0} \quad \theta = \frac{T-T_0}{T_{in}-T_0} \quad P = \frac{P-P_0}{\rho_0 u_0^2} \quad (17)$$

4. Numerical solution

The mass and energy balances on an element of falling film were developed. Because the temperature, mass fraction and velocity were known at each iteration of the gas phase, the energy conservation equation was solved. The values of temperature and water mass flow rate at each height, z, updated the boundary conditions for the vapour phase.

Dimensionless forms of Eqs. (1)–(5) were solved by the finite volume method developed by Patankar [18]. The power scheme was used to approximate the convection–diffusion terms. A main grid was adopted for the unknown scalar variables, such as temperature, mass fraction and pressure; while a staggered grid was chosen for the velocity components. The calculation domain was mapped with rectangular grids refined in both directions to ensure a more accurate modelling of heat and mass transfer. The SIMPLE algorithm was used for velocity–pressure coupling. The resulting algebraic system was solved iteratively using the line-by-line TDMA algorithm. A convergence criterion equal to 10^{-5} was chosen to determine when the problem was solved. The computing code was written in Fortran. This programme was validated by comparing our results with those of [8]. Fig. 3 shows the variation of the latent heat Nusselt number along the liquid–vapour interface. The latent heat Nusselt number was defined by the following expression:

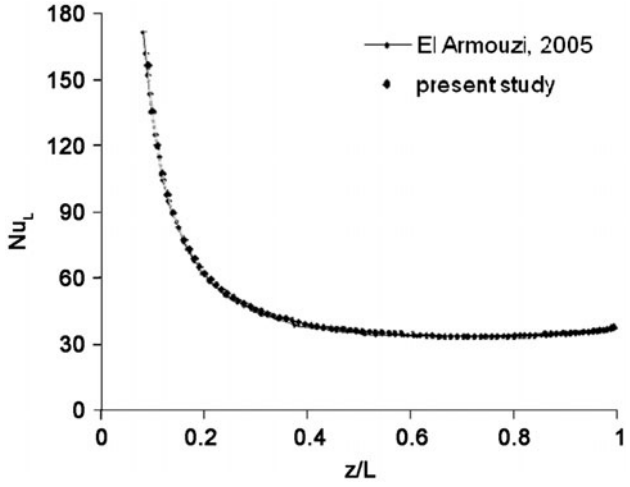

Fig. 3. Comparison of the distribution of the latent heat Nusselt number along the liquid-vapour interface for the current code calculations and for the results of El Armouzi [8].

$$Nu_L = \frac{m_v L_v}{\frac{\lambda}{d_h}(T_I - T_m)} \tag{18}$$

where T_m is the average temperature of the air-vapour mixture in the gas phase defined as:

$$T_m = \frac{\int_{R_1}^{R_2} \rho C_p ruTdr}{\int_{R_1}^{R_2} \rho C_p rudr} \tag{19}$$

This code demonstrated excellent agreement with the results of [8], illustrating that the described procedure can reproduce results previously established in the literature.

5. Results and discussion

The results of liquid film evaporation are presented to study the influence of air and water flow parameters on the average evaporated mass flux density, m_v. This parameter characterises the evaporator production and was defined as:

$$m_v = \frac{1}{L}\int_0^L m_{v,I}(z)dz \tag{20}$$

At various feed air temperatures T_0, m_v decreased linearly with respect to the mass fraction of the feed air c_0 as shown by Fig. 4. As the air flow gains moisture, the evaporation decreased weakly. Average evaporated mass flux density was divided by a factor greater than 2 as mass fraction varied from 0.5 to $20\,10^{-3}$. This result was also found by [19].

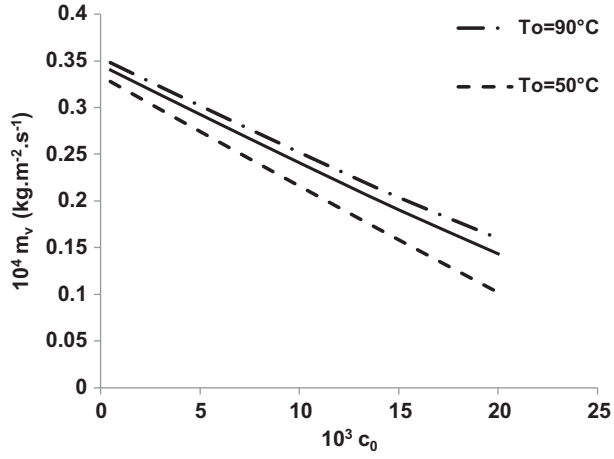

Fig. 4. Influence of the feed air mass fraction on the average evaporated mass flux density for various feed air temperatures ($u_0 = 0.8\,\mathrm{m\,s^{-1}}$, $F_{in} = 0.3\,10^{-3}\,\mathrm{kg\,s^{-1}}$, $T_{in} = 303\,\mathrm{K}$).

The feed air temperature at the inlet was the important parameter that caused evaporation; therefore, the increase in T_0 increased m_v because the air flow preheated the film. This observation is demonstrated in Fig. 5, where m_v increases with T_0. Consequently, the average evaporated mass flux density was greater than $0.34\,10^{-4}\,\mathrm{kg\,m^{-2}\,s^{-1}}$ at $T_0 = 90$°C and $c_0 = 0.5\,10^{-3}$. The result was that the evaporation was more significant when the air flow was blown at a high temperature and at a low mass fraction.

The evaporated mass flux density was compared to the air velocity u_0 for different mass fractions. The results plotted in Fig. 6 show that m_v increases with u_0.

Fig. 6 also shows that as u_0 increased m_v and thus evaporator production also increased. Additionally,

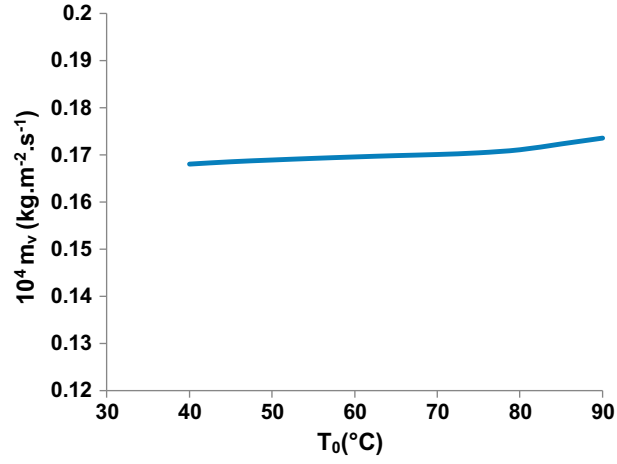

Fig. 5. Influence of the feed air temperature on the average evaporated mass flux density ($u_0 = 0.7\,\mathrm{m\,s^{-1}}$, $F_{in} = 0.4\,10^{-3}$ $\mathrm{kg\,s^{-1}}$, $c_0 = 0.5\,10^{-3}$, $T_{in} = 298\,\mathrm{K}$).

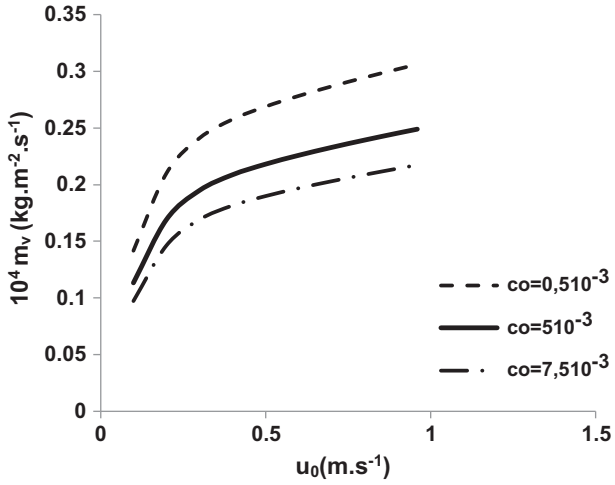

Fig. 6. Influence of the feed air velocity on the average evaporated mass flux density for different feed air mass fractions of feed air ($T_0 = 333\,K$, $F_{in} = 0.4\,10^{-3}\,kg\,s^{-1}$, $T_{in} = 300\,K$).

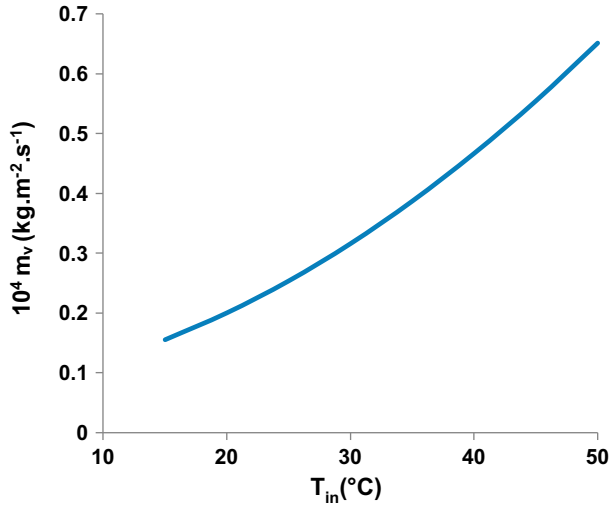

Fig. 8. Influence of the feedwater temperature on the average evaporated mass flux density ($T_0 = 328\,K$, $c_0 = 0.5\,10^{-3}$, $F_{in} = 0.25\,10^{-3}\,kg\,s^{-1}$, $u_0 = 0.7\,m\,s^{-1}$).

lower c_0 produced greater m_v at equivalent feed air velocities. At high feed air velocity and low mass fraction, the average mass flux density exceeded $0.3\,10^{-4}\,kg\,m^{-2}\,s^{-1}$.

The influence of the mass flow rate of feedwater F_{in} on the average evaporated mass flux density was also studied. Fig. 7 shows that m_v decreased with F_{in}. In fact, evaporation was pronounced for low F_{in} in order to comply with energy conservation (Eq. (9)). Conversely, because the energy that had been removed by the film increased with F_{in}, the latent heat flux must decrease.

The influence of the feedwater temperature T_{in} on m_v is illustrated in Fig. 8. The average evaporated mass flux density increased nearly linearly with increasing feedwater temperature. In fact, m_v increased by more than a factor of 4 as T_{in} varied between 15 and 50°C. Consequently, to improve liquid film evaporation, the process should be operated with a high feedwater temperature.

Because evaporation takes place in a vertical annulus, the curvature effects are important. In the limit as curvature approaches zero, a plane plate or cartesian configuration is reached. To justify the selection of an annular geometry, the curvature parameter must be studied.

We varied the inner radius R_1 and fixed all others parameters to examine the effect of curvature on m_v.

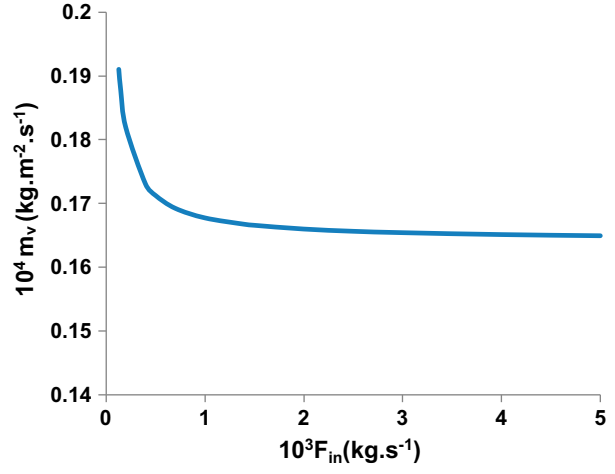

Fig. 7. Influence of the mass flow rate of feedwater on the average evaporated mass flux density ($T_0 = 333.15\,K$, $c_0 = 0.5\,10^{-3}$, $T_{in} = 290\,K$, $u_0 = 0.8\,m\,s^{-1}$).

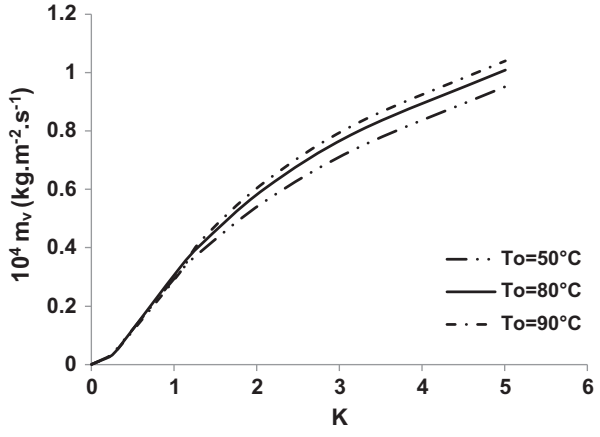

Fig. 9. Influence of the curvature on the average evaporated mass flux density for different feed air temperatures ($u_0 = 0.4\,m\,s^{-1}$, $c_0 = 0.5\,10^{-3}$, $F_{in} = 0.3\,10^{-3}$ $kg\,s^{-1}$, $T_{in} = 300\,K$).

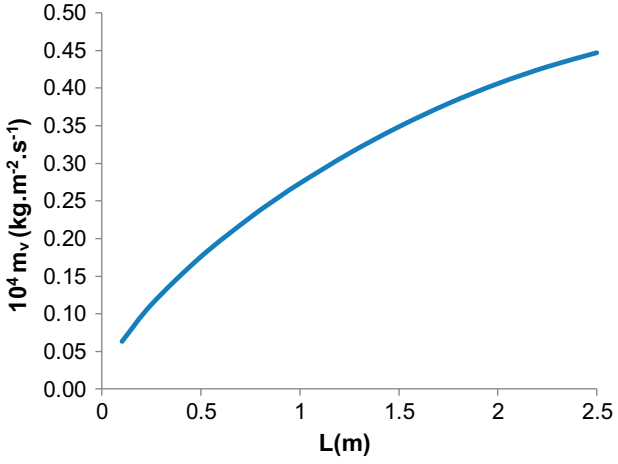

Fig. 10. Influence of the length on the average evaporated mass flux density ($u_0 = 0.4\,\mathrm{m\,s^{-1}}$, $c_0 = 0.5\,10^{-3}$, $T_0 = 333\,\mathrm{K}$, $F_{in} = 0.3\,10^{-3}\,\mathrm{kg\,s^{-1}}$, $T_{in} = 300\,\mathrm{K}$).

For several feed air temperatures, the variation of m_v with respect to the curvature K is presented in Fig. 9. Increasing curvature strongly enhanced m_v. Additionally, higher T_0 also increased the average evaporated mass flux density, as previously shown in Fig. 4. For large K and high T_0, m_v exceeded $10^{-4}\,\mathrm{kg\,m^{-2}\,s^{-1}}$.

The variation of the average evaporated mass flux density with respect to the length L is shown in Fig. 10. Similar to the profile shown in Fig. 9, the increase in length caused a pronounced evaporation enhancement.

6. Conclusion

A parametric study of the evaporation of a liquid water film falling into preheated air with mixed convection conditions considering both heat and mass transfer was conducted. The results from this computational study showed that evaporation was enhanced by increasing temperature and velocity or by decreasing the feed air mass fraction. In other words, when the air flow was supplied at a relatively high temperature and velocity with a small mass fraction, the average evaporated mass flux density was substantial. The water parameters were also examined. Evaporation enhancement was obtained by increasing the feedwater temperature and decreasing the feedwater mass flow rate. The curvature and length of the annulus were also shown to improve the evaporation rate. A better understanding of the effect of geometric parameters will enhance the performance of the evaporation system through optimization of the annular geometry.

Symbols

c — mass fraction
C — dimensionless mass fraction of vapour
Cp — heat capacity, $\mathrm{J\,kg^{-1}\,K^{-1}}$
d_h — hydraulic diameter, m
D — mass diffusivity, $\mathrm{m^2\,s^{-1}}$
F — mass flow rate of feed water, $\mathrm{kg\,s^{-1}}$
F — water mass flow rate per unit perimeter, $\mathrm{kg\,s^{-1}\,m^{-1}}$
Gr_M — mass Grashoff number
Gr_T — thermal Grashoff number
K — curvature, $K = (R_2 - R_1)/R_1$
L — length of the space, m
L_v — latent heat of vaporisation, $\mathrm{J\,kg^{-1}}$
m_v — evaporated average mass flux density referred to internal wall area, $\mathrm{kg\,m^{-2}\,s^{-1}}$
M — molecular weight, $\mathrm{kg\,mol^{-1}}$
P — pressure, Pa
q_{cv} — convective heat flux density, $\mathrm{W\,m^{-2}}$
q_L — latent heat flux density, $\mathrm{W\,m^{-2}}$
r — radial coordinate, m
R_1 — outer radius of the first cylinder, m
R_2 — inner radius of the second cylinder, m
T — temperature, K or ℃
U — axial velocity, $\mathrm{m\,s^{-1}}$
v — radial velocity, $\mathrm{m\,s^{-1}}$
U — dimensionless axial velocity
V — dimensionless radial velocity
Z — axial coordinate, m

Greek

λ — thermal conductivity, $\mathrm{W\,m^{-1}\,K^{-1}}$
μ — dynamic viscosity, $\mathrm{kg\,m^{-1}\,s^{-1}}$
η — dimensionless radial coordinate, $\eta = r/R_2$
ρ — density, $\mathrm{kg\,m^{-3}}$
θ — dimensionless temperature
ζ — dimensionless axial coordinate

Subscripts

a — air
in — of feedwater
I — at the interface
l — liquid
out — outlet of water
v — vapour
s — outlet of air
0 — inlet of air

References

[1] W.M. Yan, Y.L. Tsay, T.F. Lin, Simultaneous heat and mass transfer in laminar mixed convection flows between vertical parallel plates with asymmetric heating, Int. J. Heat Fluid Flow 10 (1989) 217–237.

[2] C. Debissi, J. Orfi, S. Ben Nasrallah, Evaporation of water by free or mixed convection into humid air or superheated steam, Int. J. Heat Mass Transfer 46 (2003) 4703–4715.
[3] Z. Ait Hammou, B. Benhamou, N. Galanis, J. Orfi, Laminar mixed convection of humid air in a vertical channel with evaporation or condensation at the wall, Int. J. Thermal Sci. 44 (2004) 531–539.
[4] W.M. Yan, H.C. Tsay, Mixed convection heat and mass transfer in vertical annuli with asymmetric heating, Int. J. Heat Mass Transfer 34 (1991) 1309–1313.
[5] W.M. Yan, D. Lin, Natural convection heat and mass transfer in vertical annuli with film evaporation and condensation, Int. J. Heat Mass Transfer 44 (2001) 1143–1151.
[6] J.H. Jang, W.M. Yan, C.C. Huang, Mixed convection heat transfer enhancement through film evaporation in inclined square ducts, Int. J. Heat Mass Transfer 48 (2005) 2117–2125.
[7] K. Fahem, S. Ben Jabrallah, A. Belghith, J.P. Corriou, Numerical simulation of the behaviour of a distillation cell with influence of the characteristics of the heating wall, Desalination 201 (2006) 185–197.
[8] M. El Armouzi, X. Chesneau, B. Zeghmati, Numerical study of evaporation by mixed convection of a binary liquid film flowing down the wall of two coaxial cylinders, Heat Mass Transfer 41 (2005) 375–386.
[9] M. Feddaoui, A. Mir, E. Belahmidi, Cocurrent turbulent mixed convection heat and mass transfer in falling film of water inside a vertical heated tube, Int. J. Heat Mass Transfer 46 (2003) 3497–3509.
[10] J.H. Jang, W.M. Yan, Thermal protection with liquid film in turbulent mixed convection channel flows, Int. J. Heat Mass Transfer 49 (2006) 3645–3654.
[11] S. Ben Jabrallah, A. Belghith, J.P. Corriou, Etude des transferts couplés de matière et de chaleur dans une cavité rectangulaire: Application à une cellule de distillation [Study of heat and mass transfer in a rectangular cavity: Application to a distillation cell], Int. J. Heat Mass Transfer 45 (2002) 891–904.
[12] A.S. Cherif, M.A. Kassim, B. Benhamou, S. Harmand, J.P. Corriou, S. Ben Jabrallah, Experimental and numerical study of mixed convection heat and mass transfer in a vertical channel with film evaporation, Int. J. Thermal Sci. 50 (2011) 942–953.
[13] K. Zhania, H. Ben Bachab, T. Damak, Study of a water desalination unit using solar energy, Desal. Water Treat. 3 (2009) 261–270.
[14] M. Abu-Arabi, H. Mousa, R. Abdelrahman, Solar desalination unit with falling film, Desal. Water Treat. 3 (2009) 58–63.
[15] C. Ziqian, Z. Hongfei, M. Chaochen, L. Zhengliang, H. Kaiyan, Experiment and optimal parameters of a solar heating system study on an absorption solar desalination unit, Desal. Water Treat. 1 (2009) 128–138.
[16] W.M. Yan, Binary diffusion and heat transfer in mixed convection pipe flows with film evaporation, Int. J. Heat Mass Transfer 36 (1993) 2115–2123.
[17] R. Ben Radhia, J.P. Corriou, S. Harmand, S. Ben Jabrallah, Numerical study of evaporation in a vertical annulus heated at the inner wall, Int. J. Thermal Sci. 50 (2011) 1996–2005.
[18] S.V. Patankar, Numerical Heat Transfer and Fluid Flow, Hemisphere, New York, 1980.
[19] C. Debbissi, J. Orfi, S. Ben Nasrallah, Evaporation of water by free convection in a vertical channel including the effects of wall radiative properties, Int. J. Heat Mass Transfer 44 (2001) 811–826.